Supplementary Methods

Vector Construction

The creation of replication-competent ASLV long terminal repeat with a splice (RCAS)-PDGFB was described previously [1]. We created RCAS-FGL2 with a V5 tag by cloning the *FGL2* cDNA from pBMN-FGL2 into a Gateway-compatible RCAS vector. The Gateway LR recombination reaction between the RCAS vector and FGL2-containing entry vector resulted in RCAS-FGL2-V5, which was verified by sequencing.

Transfection of DF-1 cells

Immortalized DF-1 chicken fibroblasts were grown in Dulbecco modified Eagle medium containing 10% fetal bovine serum in a humidified atmosphere (95% air and 5% carbon dioxide) at 37°C. Live virus was produced by transfecting the RCAS vector into DF-1 cells using FuGENE-6 (Roche, Indianapolis, IN) and allowing the cells to replicate in culture. We used immunofluorescence and V5-probe antibody for Western Blot (sc-81594, Santa Cruz Biotechnology, Dallas, Tx) to verify FGL2 expression in DF-1 cells infected with RCAS-FGL2-V5. Untransfected DF-1 cells were used as a negative control.

Clustered regularly interspaced short palindromic repeats–mediated inhibition of FGL2 expression in GL261 cells

Mouse FGL2 guide RNA sequences GCTGCCGCACTGCAAGGATG and GTGCTCCTCCACCGCTCGGC were cloned into the pX458 vector for CRISPR associated protein 9 and guide RNA expression (provided by Dr. Feng Zhang and colleagues at the Massachusetts Institute of Technology [Cambridge, MA]. GL261 cells were transfected with both

guide plasmids, the cells were grown for 2 weeks, and green fluorescent protein–positive cells were isolated. The knockdown of FGL2 expression in the GL261 cells was confirmed by quantitative polymerase chain reaction, which was amplified with the following primers: forward, TCTGGGAACTGTGGGCTCTATT, and reverse, AGTTGGCAGAGAGACATGAATCAA. GAPDH was used as control, primer forward, CCAGCCTCGTCCCGTAGAC, and reverse, CGCCCAATACGGCCAAA.

GL261 mouse model

For the orthotopic glioblastoma mouse model, cultured GL261-mock or GL261-FGL2 knockout (GL261-FGL2KO) cells were collected in logarithmic growth phase, washed twice with PBS, and mixed with an equal volume of 3% methylcellulose in PBS. Cells (5×10^4 in a total volume of 5 μL) were intracerebrally injected in C57/BL6 mice (N=8 for each group). Mice were observed daily. When the mice showed signs of neurological compromise, they were humanely euthanized.

Ntv-a mouse model

DF-1 producer cells transfected with RCAS vector (1×10^4 cells in 1–2 μL of phosphate-buffered saline solution [PBS]) were injected bilaterally into the frontal lobes of mice with a 10-μL gas-tight Hamilton syringe. The mice were injected within 24–72 h after birth when Nestin-positive cells producing avian tumor virus receptor A are most proliferative. Equal amounts of DF-1 cells were injected in mice to generate the RCAS-FGL2 (n=15), RCAS-PDGFB (n=34), and RCAS-PDGFB+RCAS-FGL2 (n=35) groups.

GSCs- Cell culture and RNA Isolation/Sequencing

Patient-derived glioma stem cells (GSCs) were described previously [2]. The GSCs were cultured in NSC proliferation media (Millipore Corporation, Billerica, MA) with 20 ng/ml EGF and 20 ng/ml bFGF. The GSCs were characterized by subtype signature using RNA sequencing for CD44, FN1, CHI3L1, CTGF (mesenchymal subtype marker) or Olig2. SOX2, SOX9, PROM1 (proneural subtype marker) as described earlier by Verhaak et al. [3]. Total RNA from 17 glioma sphere-forming cells was isolated using the Masterpure complete DNA and RNA isolation kit (Epicenter, Madison, WI) after proteinase K digestion, following the manufacturer's instructions. Paired-end sequencing of the RNA was performed using the Illumina HiSeq2000 sequencer at the University of Texas M.D Anderson Cancer Center Sequencing and Microarray Facility (SMF). An average of 55 million paired-ends were generated for each of the GSCs. Sequence reads were aligned to protein-coding genes according to Ensembl reference transcriptome (version 64) and RPKM (reads per kilobase per million reads) values were generated using the Pipeline for RNA sequencing Data Analysis (PRADA)[4]

Western Blot Analysis

Verification of FGL2 expression in GSCs was performed by Western blotting as described earlier [2]. Protein samples (10 μg) were fractionated by sodium dodecyl sulfate polyacrylamide gel electrophoresis using gels containing 10% polyacrylamide, transferred to a polyvinylidene difluoride membrane, and probed with the anti-FGL2 antibody (H00010875-M01, 1:1000; Abnova, Taiwan) to detect FGL2 expression and β-actin HRP (1:10,000; Santa Cruz Biotechnology, Dallas,

TX) was used for the loading control. Goat anti-rabbit IgG (1:10,000; Santa Cruz Biotechnology, Dallas,TX) was used as the secondary antibody. The blots were developed using the ECL Plus detection kit (GE Healthcare) following the manufacturer's protocol.

Enzyme-linked immunosorbent assay

GSCs pellets were subjected to cell culture lysis buffer (Promega) plus protease inhibitors. Cell lysates (20 μg of protein per well) were loaded on a pre-coated anti-FGL2 enzyme-linked immunosorbent assay (ELISA) plate. FGL2 expression levels were detected using ELISA kits according to the manufacturer's instructions (LEGEND MAX Human FGL2 ELISA Kit, catalog: 436907; BioLegend, San Diego, CA).

Flow cytometry

Mouse brain tissues were minced and enzymatically digested to obtain single-cell suspensions. Brain-infiltrating lymphocytes were isolated according to a previously published protocol [5]. Briefly, each single-cell suspension was centrifuged through a 30% Percoll gradient at 7800 *g* for 30 min. The lymphocyte layer was collected, centrifuged, and washed. Cell-surface staining was performed with fluorescein isothiocyanate and phycoerythrin-labeled anti-CD4 antibody (mouse monoclonal1:50; BioLegend, San Diego, CA). For intracellular staining, cells were fixed and permeabilized and were incubated with PerCP/Cy5.5–labeled anti-FoxP3 antibody (mouse monoclonal, 1:25; BioLegend, San Diego, CA). Stained cells were analyzed using flow cytometry and FlowJo software (FlowJo LLC, Ashland, OR).

IHC and immunofluorescence

Mouse brains were formalin-fixed and paraffin-embedded, and 4-μm sections were used for IHC. The Lab VisionPT Module (Thermo Fisher Scientific) with citrate buffer was used for antigen retrieval. Sections of human glioma tissue were antigen-retrieved by Antigen Retrieval Acidic solution (R&D, CTS014). Staining was performed using the Lab Vision Immunohistochemical Autostainer 360-2D (Thermo Fisher Scientific). Immunoreactive staining was visualized using an avidin-biotin complex technique, with 3,3'-diaminobenzidine (Invitrogen) as the chromogenic substrate and hematoxylin as the counterstain. The following antibodies were used for IHC: V5 (sc 81594, 1:50 dilution, Santa Cruz Biotechnology, Dallas, TX); CD44 (ab41478, 1:100, Abcam, Cambridge, MA); Olig2 (AB9610,1:500, EMD Millipore, Burlington, MA); FoxP3 (NB100-39002, 1:400, Novus Biologicals, Littleton, CO); Iba1 (NBP2-16908, 1:1000¸ Novus Biologicals, Littleton, CO); CD68 (SM1550PS, 1:300, Acris, Rockville, MS); and CD11b/c (NB110-40766, 1:400, Novus Biologicals, Littleton, CO). We counted the total number of cells and the number of positively stained cells in the areas of highest tumor cell density in 5-6 non-overlapping microscopic fields (magnification, 400×) in tumor-bearing brains taken from mice in each group. We counted 15 tumors for the FGL2-HGG and PDGF-LGG group and 9 tumors for the FGL2-LGG and 9 tumors for the PDGF-HGG group.

For double immunofluorescence staining to detect microglia, tumor sections were stained with mouse anti-Iba1 antibody (MABN92, 1:100, Millipore, Burlington, MA) and rabbit-arginase 1 (Arg1) Alexa Fluor 555–conjugated antibody (bs-8585R-555, Bioss Inc. Woburn, MA) overnight at 4°C, followed by 1 h incubation with goat anti-mouse Alexa Fluor 488–conjugated antibody (1:500, Invitrogen, Carlsbad, CA). ProLong Gold Antifade Mountant with 4'-diamidino-2-phenylindole (DAPI; Thermo Fisher Scientific, Waltham, MA) was used as the mounting medium. Slides were further processed for imaging and confocal analysis using an Olympus

Fluoview FV1000 microscope. We quantified the percentage of positive cells (yellow) by counting the number of cells that stained for both Iba1 and Arginase 1 in at least five non-overlapping microscopic fields (magnification, 400× and/or 600×) from each genotype. The number of positive cells was divided by the total number of $DAPI^+$ cells.

Ethical Statements:

All applicable international, national, and/or institutional guidelines for the care and use of animals were followed. All procedures performed in studies involving animals were in accordance with the ethical standards of the institution or practice at which the studies were conducted. All procedures performed in studies involving human participants were in accordance with the ethical standards of the institutional and/or national research committee and with the 1964 Helsinki declaration and its later amendments or comparable ethical standards.

References

1. Dai C, Celestino JC, Okada Y, *et al.* PDGF autocrine stimulation dedifferentiates cultured astrocytes and induces oligodendrogliomas and oligoastrocytomas from neural progenitors and astrocytes in vivo. Genes Dev 2001;15(15):1913-25.
2. Bhat KP, Salazar KL, Balasubramaniyan V, *et al.* The transcriptional coactivator TAZ regulates mesenchymal differentiation in malignant glioma. Genes Dev 2011;25(24):2594-609.
3. Verhaak RG, Hoadley KA, Purdom E, *et al.* Integrated genomic analysis identifies clinically relevant subtypes of glioblastoma characterized by abnormalities in PDGFRA, IDH1, EGFR, and NF1. Cancer Cell 2010;17(1):98-110.
4. Torres-Garcia W, Zheng S, Sivachenko A, *et al.* PRADA: pipeline for RNA sequencing data analysis. Bioinformatics 2014;30(15):2224-6.
5. LaFrance-Corey RG, Howe CL. Isolation of brain-infiltrating leukocytes. J Vis Exp 2011; 10.3791/2747(52).

Supplementary Table 1. Distribution of FGL2over and FGL2low expressing cases.

	$FGL2^{over}$	$FGL2^{low}$
HGG	77	61
LGG	36	49

IDH WT Gliomas (N=609). Fisher's exact test, p=0.054

	$FGL2^{over}$	$FGL2^{low}$
MUT	159	210
WT	72	14

LGGs (N=457). Fisher's exact test, p<0.001

	$FGL2^{over}$	$FGL2^{low}$
Codel	46	104
Non-Codel	145	81

All IDH MUT gliomas. Fisher's exact test, p<0.001

Supplementary Table 2: LGG-HGG matched samples. CT= chemotherapy, RT= radiotherapy, *at initial diagnosis, #after initial diagnosis.

LGG-HGG Sample no.	Pathology	CoDel	IDH Status	Age*	KPS*	Treatment#	Time to Progression
1	Oligodendroglioma	Yes	Mut	29	100	CT,RT	9 years
2	Oligodendroglioma	Yes	Unknown	24	100	CT	7 years
3	Oligodendroglioma	Yes	Unknown	37	100	None	6 years
4	Oligodendroglioma	Yes	Unknown	34	100	CT	7 years
5	Oligodendroglioma	Yes	Unknown	48	90	CT	5 years
6	Oligodendroglioma	Yes	Mut	33	100	None	6 years
7	Astrocytoma	No	WT	30	100	RT	7 years
8	Oligodendroglioma	Yes	Mut	29	100	CT	4 years
9	Astrocytoma	Yes	Mut	32	100	RT	6 years
10	Astrocytoma	No	Mut	31	100	RT	4 years

Supplementary Table 3. Tumor grade and Histology of tumors formed in RCAS-PDGF+FGL2 injected mice. MVP: microvascular proliferation; N: no tumor observed.

Sample	Tumor Grade	Pathology
1	HGG	MVP
2	HGG	MVP, necrosis
3	HGG	MVP, necrosis
4	LGG	-
5	LGG	-
6	HGG	MVP
7	HGG	MVP, necrosis
8	HGG	MVP
9	HGG	MVP
10	HGG	MVP, necrosis
11	HGG	MVP, necrosis
12	LGG	-
13	HGG	MVP
14	LGG	-
15	N	-
16	LGG	-
17	N	-
18	HGG	MVP
19	HGG	MVP
20	LGG	-
21	LGG	-
22	HGG	MVP
23	HGG	MVP
24	HGG	MVP, necrosis
25	HGG	MVP, necrosis
26	HGG	MVP
27	HGG	MVP, necrosis
28	N	-
29	HGG	MVP
30	LGG	-
31	HGG	MVP, necrosis
32	HGG	MVP, necrosis
33	HGG	MVP, necrosis
34	HGG	MVP, necrosis
35	HGG	MVP, necrosis
36	LGG	-
37	N	-

Supplementary Table 4.Tumor grade and Histology of tumors formed in RCAS-PDGF injected mice. MVP: microvascular proliferation; N: no tumor observed

Sample	Tumor Grade	Pathology
1	HGG	MVP, necrosis
2	LGG	-
3	HGG	MVP, necrosis
4	HGG	MVP
5	N	-
6	LGG	-
7	HGG	MVP, necrosis
8	LGG	-
9	LGG	-
10	LGG	-
11	LGG	-
12	LGG	-
13	LGG	-
14	LGG	-
15	HGG	MVP
16	LGG	-
17	LGG	-
18	HGG	MVP
19	LGG	-
20	LGG	-
21	HGG	MVP, necrosis
22	LGG	-
23	LGG	-
24	HGG	MVP
25	LGG	-
26	LGG	-
27	LGG	-
28	HGG	MVP, necrosis
29	LGG	-
30	LGG	-
31	LGG	-
32	LGG	-

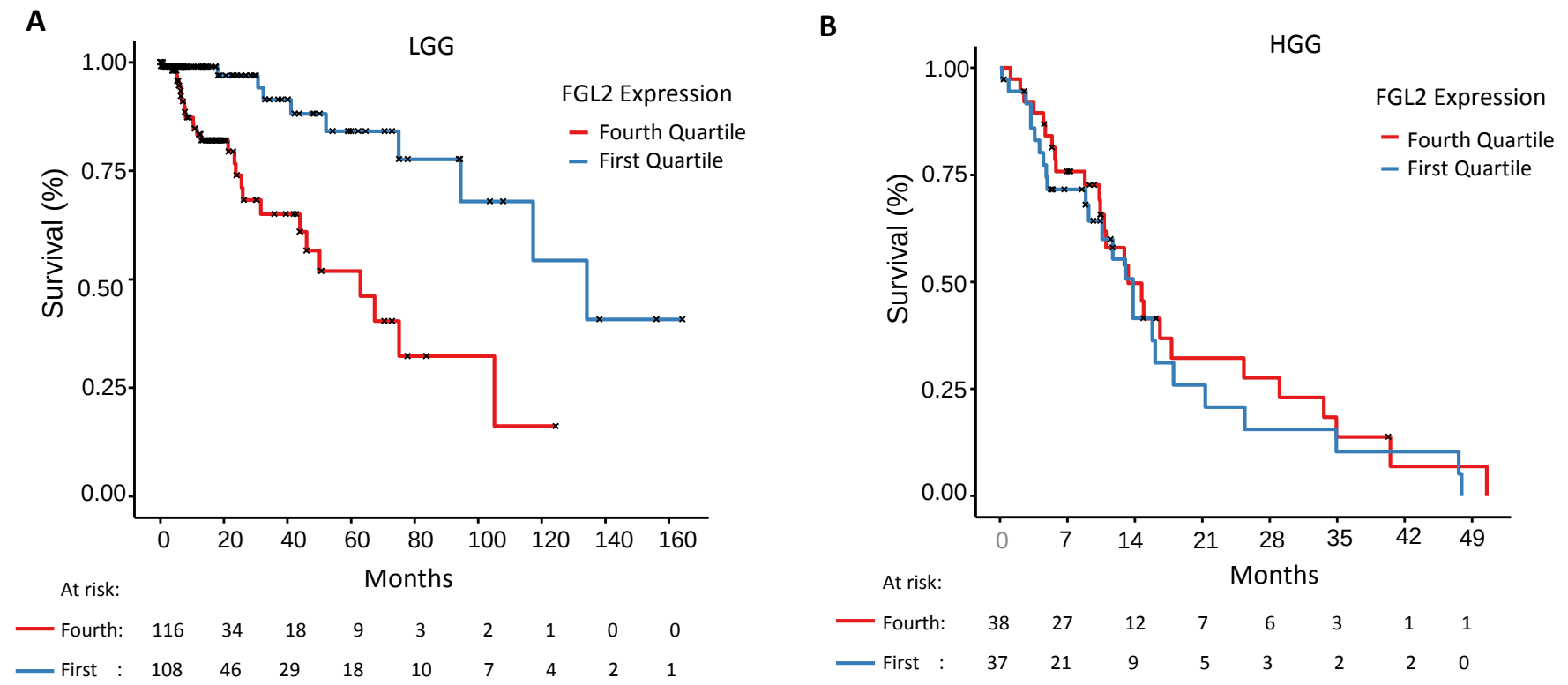

Supplementary Figure 1. The Cancer Genome Atlas dataset analysis of FGL2 expression in (**A**) LGG (N=224, Log rank test p<0.001) and (**B**)HGG (N=75, Log rank test p=0.51) in first and fourth quartiles of FGL2 expression. LGG (low-grade glioma), HGG (High-grade glioma).

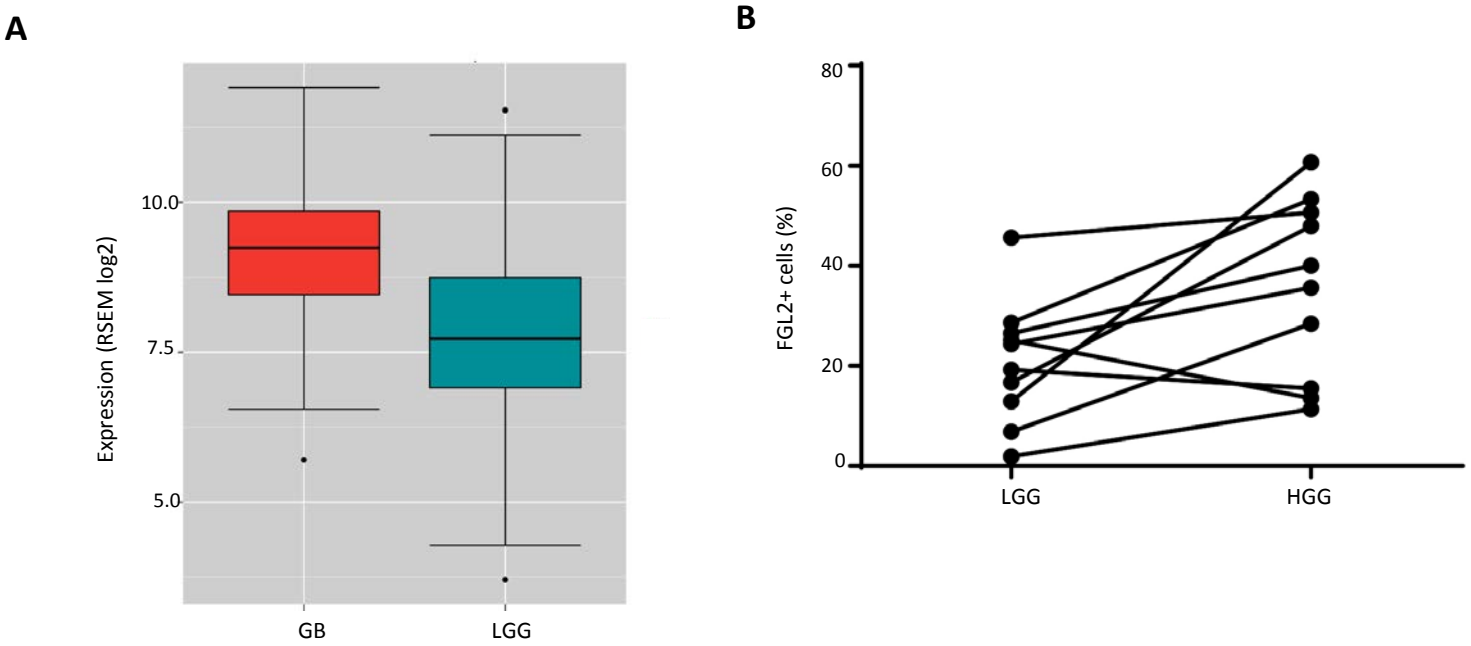

Supplementary Figure 2. FGL2 expression in glioma. **A**. Increased FGL2 expression in glioblastoma compared with low-grade glioma in the diffuse glioma, The Cancer Genome Atlas dataset. **B.** Scatter plot demonstrating significantly increased FGL2 expression in 8/10 matched samples of LGG and HGG from patients (T-test, two sided, p=0.02). LGG (low-grade glioma), HGG (High-grade glioma).

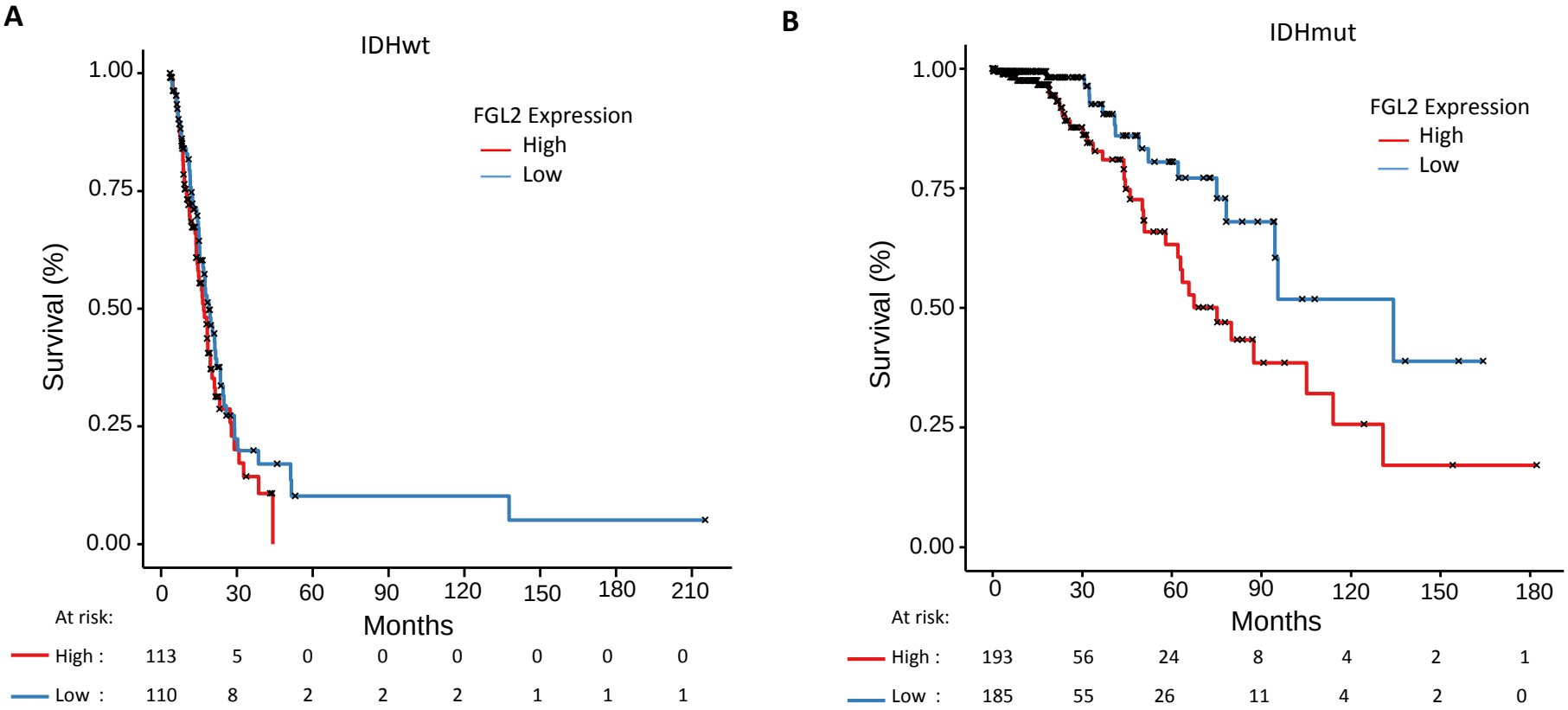

Supplementary Figure 3. The Cancer Genome Atlas dataset analysis of Median Survival showing FGL2 expression in (**A**) All IDHwt gliomas (N=223, log rank test, p=0.19), (**B**) All IDHmut gliomas (N=378, log rank test, p=0.008).

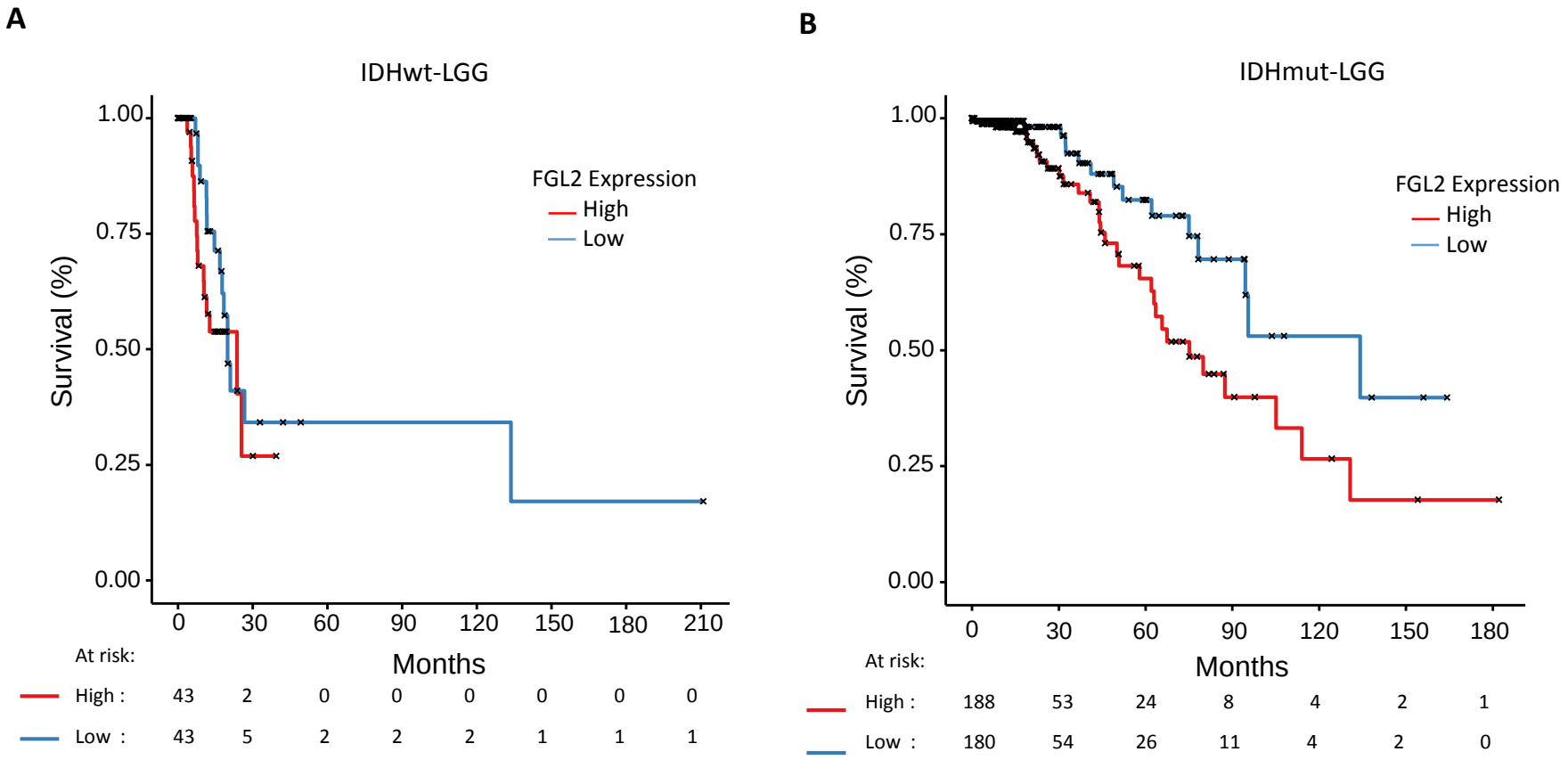

Supplementary Figure 4. The Cancer Genome Atlas dataset analysis of Median Survival showing FGL2 expression in (**A**) IDHwt-LGG (N=86, log rank test, p=0.24), (**B**) IDHmut-LGG (N=368, log rank test, p=0.01).

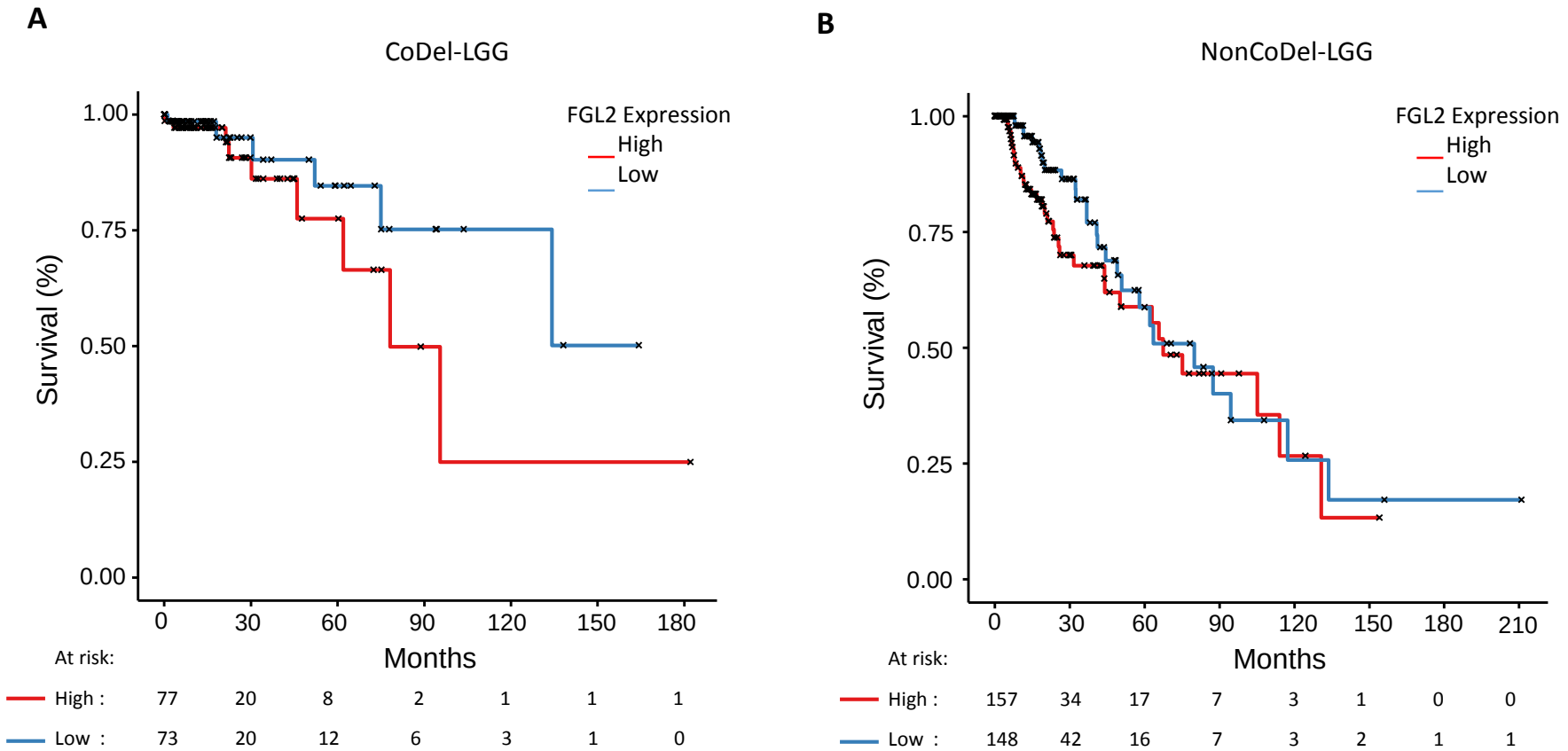

Supplementary Figure 5. The Cancer Genome Atlas dataset analysis of Median Survival showing FGL2 expression in (**A**,**B**) IDHmut LGG cases with 1p/19Q chromosomes (either co-deleted (CoDel) (N=150, log rank test, p=0.20) or non-codeleted (NonCoDel) (N=305, log rank test, p=0.12).

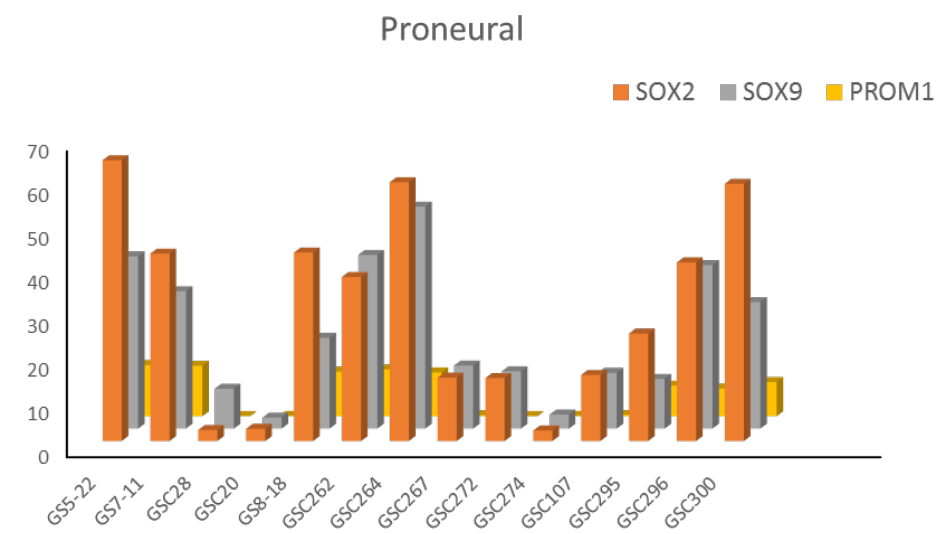

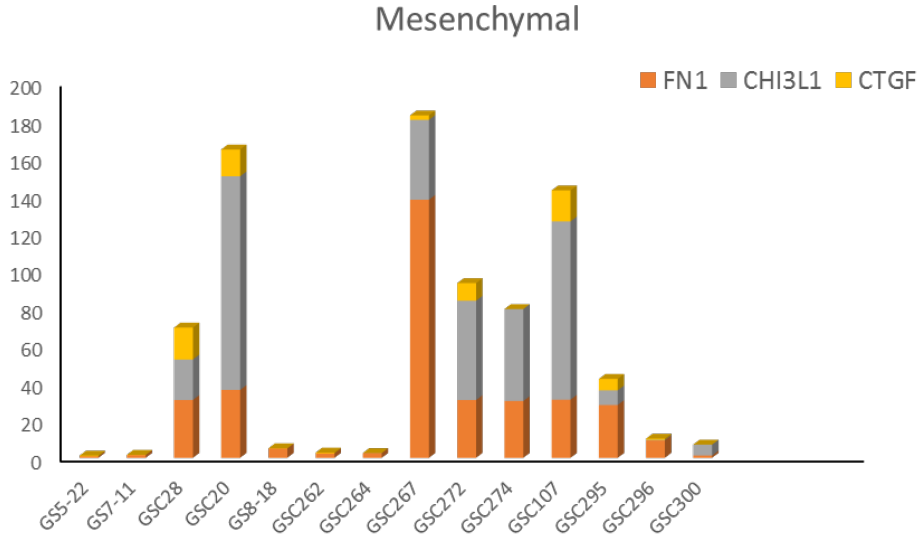

Supplementary Figure 6. Proneural (PN) and Mesenchymal (MES) marker characterization of the GSCs. Stacked bar graph showing characterization of PN and MES GSC cell lines using PN markers, SOX2, SOX9, and PROM1 and MES markers, FN1, CHI3L1, and CTGF**.** GSCs (Glioma Stem Cells).

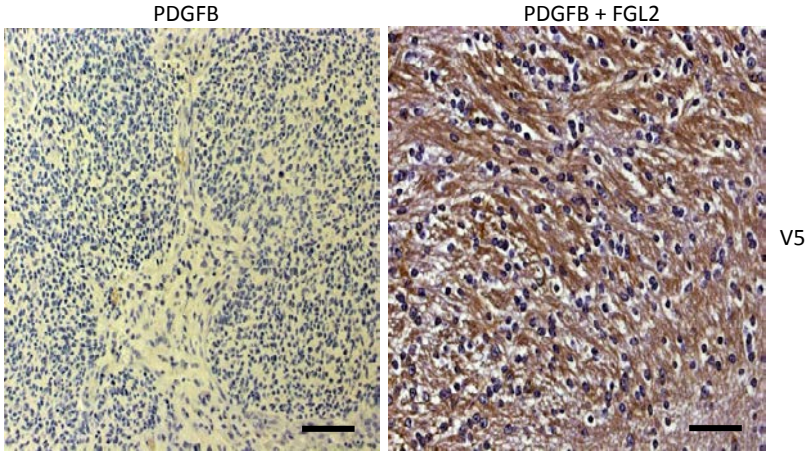

Supplementary Figure 7. Fibrinogen-like protein 2 (FGL2) expression detected by V5 staining in both RCAS-PDGFB+FGL2 and RCAS-PDGFB tumors (magnification, 400×; scale bar=50 μm).

A

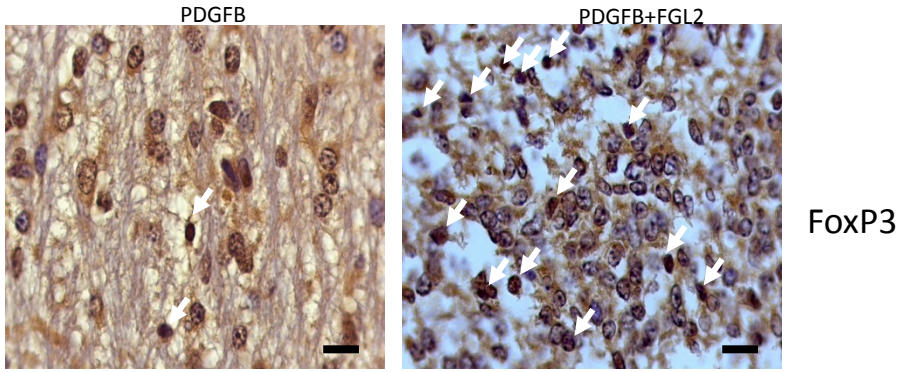

B

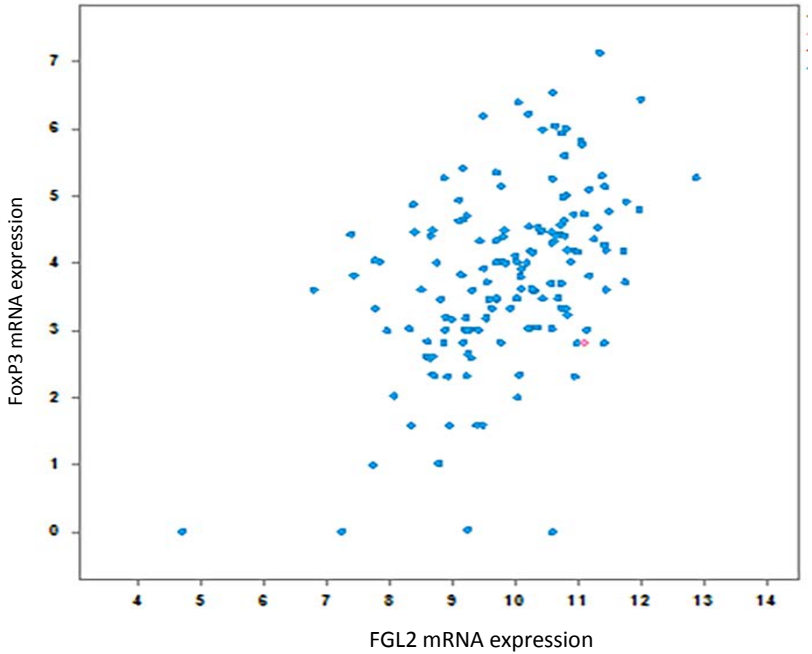

Supplementary Figure 8. A. Forkhead box P3 (FoxP3)-positive cells (magnification, 1000×; scale bar = 50μm) in representative tumors induced by RCAS-PDGFB alone or PDGFB+ FGL2. Arrows indicate positive nuclear staining of FoxP3. **B.** Analysis of The Cancer Genome Atlas data showed significant co-occurrence of FGL2 and FOXP3 mRNA (log OR 1.62, Fisher's exact test, $p<0.001$).

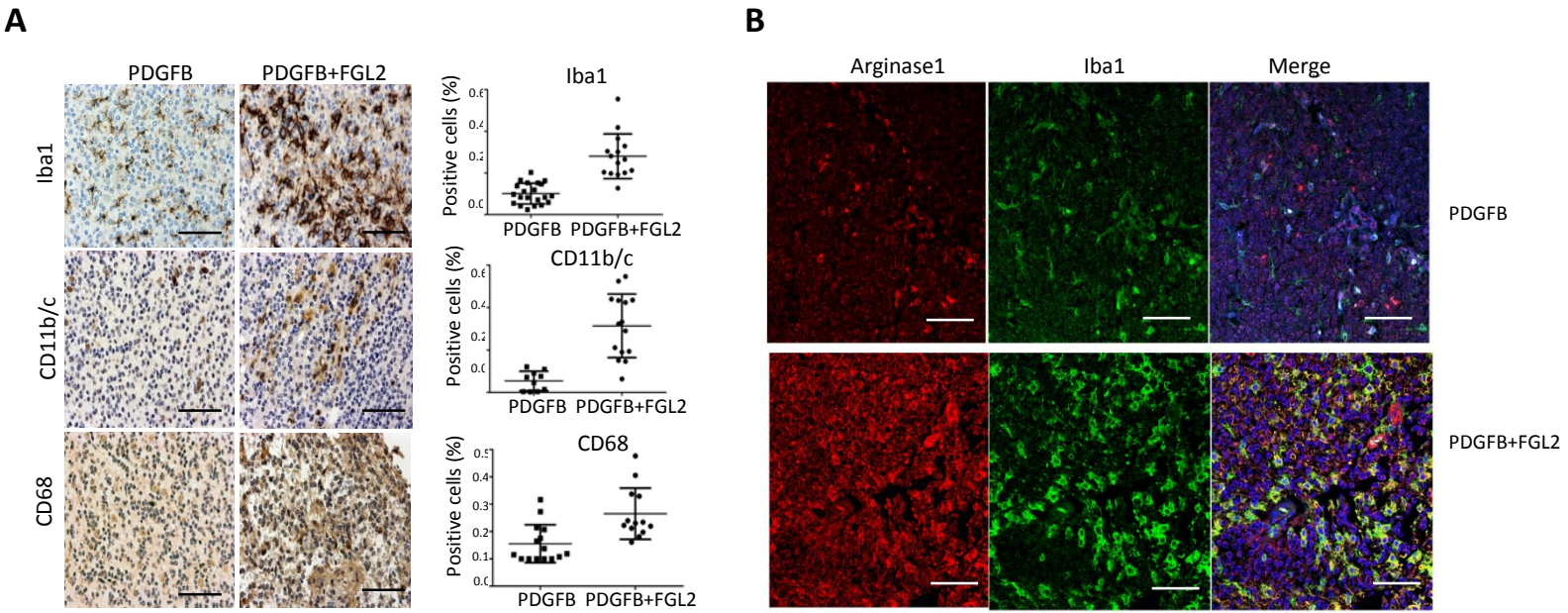

Supplementary Figure 9. A. Expression of macrophage markers Iba1, CD11b/c, and CD68) in representative RCAS-PDGFB and RCAS-PDGFB+FGL2 tumors (magnification, 400×; scale bar=50 µm). Scatter plots show increased macrophages in the RCAS-PDGFB+FGL2 tumors compared to RCAS-PDGFB tumors. For IBA1 $p<0.001$, for CD11b/c $p<0.001$, for CD68 $p=0.001$(T test, two-sided). **B**. Expression of Arginase 1+/Iba1^{+} cells in the RCAS- PDGFB+FGL2 and RCAS-PDGFB tumors indicating M2 polarization. Representative immunofluorescence staining for Arginase 1 (red) and Iba1 (green) macrophages in both cohorts (magnification, 400×; scale bar=50 µm).

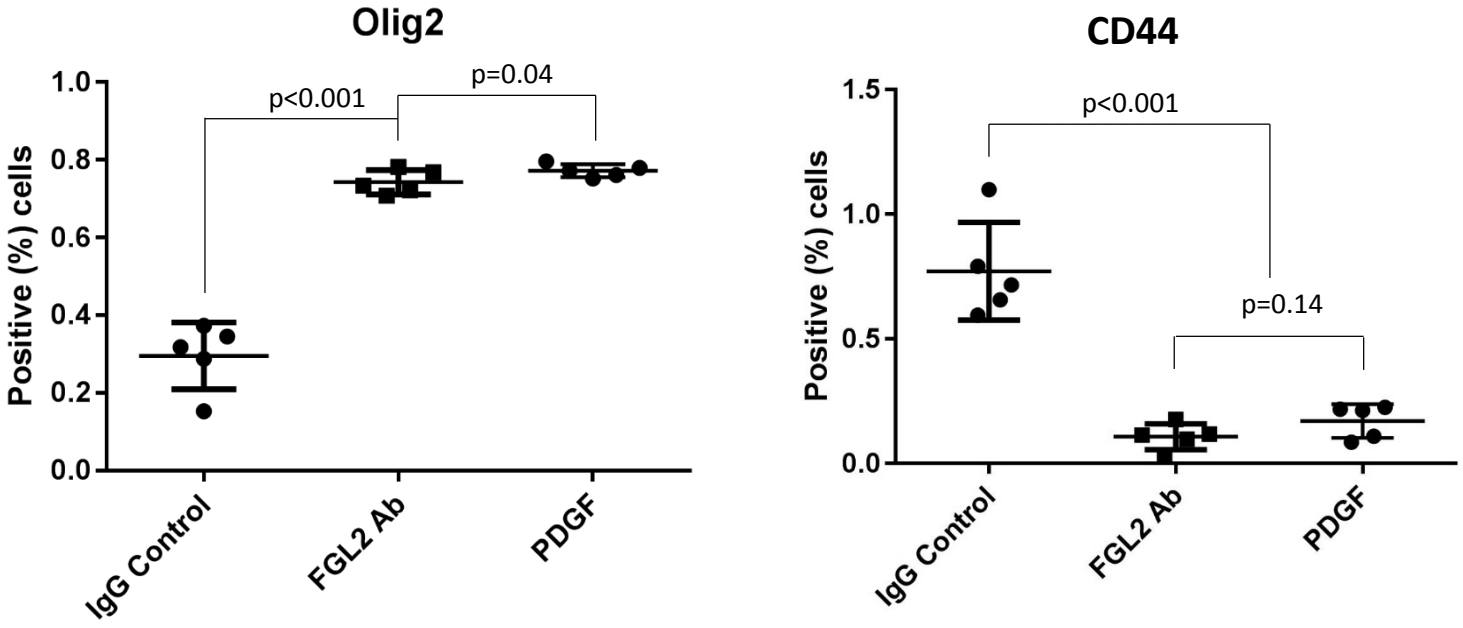

Supplementary Figure 10. Scatter plot (T test, two-sided) showing significant difference in Olig2 and CD44 levels between the IgG control and FGL2-Ab treated mice and no significant difference in Olig2 and CD44 expression between the FGL2-Ab treated mice and RCAS-PDGF group.